Proceedings of the 21st ICSMGE, Vienna, Austria, 14 – 19 June 2026. Pistrol, Adam & Schweiger (eds.)
Published by: ÖGG, Austrian Society for Geomechanics, Salzburg, Austria, ISBN 978-3-9503898-4-5
https://doi.org/10.53243/ICSMGE2026-1886

Vertical acceleration and directionality effects on the seismic response of a slope

Ángel A. Morales, Miguel A. Mánica
Institute of Engineering, National Autonomous University of Mexico, Mexico City, Mexico,
augustomoralestapia@outlook.com

Luis A. Pinzón
Scientific and Technological Research Center, Universidad Católica Santa María La Antigua, Panama City, Panama.

ABSTRACT: Due to their inherent asymmetry, slopes are particularly prone to directionality effects, understood as variations in seismic response with respect to azimuthal orientation. Although this issue has recently gained attention and its significance is now well recognised, several aspects remain insufficiently understood. Among them, the influence of the vertical component of ground motions on the response of slopes stands out as particularly relevant, both in terms of its direct effect on displacements and its interplay with directionality. This study explores this aspect using a rigid-block model that simultaneously considers the effects of the horizontal and vertical components on both the driving force and the shear strength at the sliding interface. Directionality was assessed through a rotational approach, allowing for a comprehensive evaluation of the slope response with respect to azimuthal orientation. Input motions were defined by 112 sets of acceleration time histories, selected according to specific criteria. Regarding the slope characteristics, different combinations of parameters were evaluated, with values considered representative of the failure mechanisms of interest. A demand-based scaling strategy was also proposed and applied to reduce dispersion and to constrain displacements within realistic bounds. Results indicate that, overall, the vertical component has a limited effect on both the magnitude of displacements and the orientation of maximum response. Nevertheless, several cases exhibited significant differences, which can be attributed to the interaction between dominant motion pulses in different directions.

KEYWORDS: Directionality Effects, Vertical Motion, Seismic Slope Stability, Rigid-Block Method, Permanent Displacements.

1 INTRODUCTION

In seismically active regions, the stability of slopes, embankments, and dams is a central concern in geotechnical engineering. Failures in these structures can severely disrupt infrastructure, cause major economic damage, and even result in loss of life. In response, a wide range of methodologies have been developed to analyse the impact of earthquakes on slopes (Jibson, 2011). Among these, the rigid-block method provides a straightforward alternative for assessing slope performance without relying on complex numerical simulations.

This approach estimates displacements through a double integration of acceleration time histories recorded during seismic events. These records are typically obtained from triaxial accelerometers measuring two horizontal components and one vertical component. However, a critical issue is the uncertainty in the direction and intensity of ground motions, which causes the system response to depend on its orientation relative to the seismic source. Therefore, the critical demand often occurs for an unknown intermediate orientation (Pinzón *et al.*, 2020). This phenomenon, commonly referred to as seismic directionality, is especially relevant in slopes due to their asymmetry and nonlinear behaviour (Morales, Manica and Pinzon, 2024).

Another important aspect in seismic slope stability analyses is the influence of the vertical component. While some studies argue that neglecting it may lead to underestimating displacements (Kramer and Lindwall, 2004; Korzec and Jankowski, 2021), others report its effects to be negligible due to compensating mechanisms within the system (Gazetas, Garini and, Georgarakos, 2009; Du, 2018). The apparent disagreement among previous studies may arise from differences in the assumptions used to model the rigid-block system and the way seismic loading is represented.

Within this context, the present work investigates alternative modelling strategies within the rigid-block framework, focusing specifically on the interaction between the vertical motion component and horizontal directionality.

2 METHODOLOGY

2.1 *Rigid block under bidirectional loading*

The classical rigid-block method, introduced by Newmark (1965), models a slope as a rigid mass resting on a planar surface with a rigid-plastic interface. When the force acting on the mass exceeds its basal resistance, the mass begins to slide and continues moving until its relative velocity with respect to the base reaches zero. The minimum seismic force required to initiate movement, expressed as an equivalent acceleration, is known as the critical or yield acceleration.

A key aspect of this approach lies in how seismic forces are represented. Newmark (1965) proposed that the horizontal acceleration acts along a fixed direction, known as the thrust angle, which depends on the geometry of the failure surface. Notably, the vertical component of seismic motion is neglected. By keeping the thrust angle constant, the method ensures that the block acceleration is always parallel to the sliding plane. This simplification implies that seismic forces do not affect the normal stress at the sliding interface, resulting in a constant critical acceleration. As highlighted by several authors (Kramer and Lindwall, 2004; Du, 2018; Korzec and Jankowski, 2021), this assumption can lead to significant underestimation of slope displacements.

To overcome these limitations, an alternative formulation that incorporates bidirectional seismic loading is proposed. Consider the simplest case of failure, an infinite slope with a planar failure surface, as illustrated in Figure 1. This configuration can be represented by a rigid block resting on a base inclined at an angle α, equal to the slope inclination (see Figure 2a).

As highlighted by Korzec and Jankowski (2021), accurately computing permanent displacements via double integration requires the use of the inertial acceleration time histories, $a'_x(t)$ and $a'_y(t)$, acting on the rigid block, for consistency with the physical phenomenon.

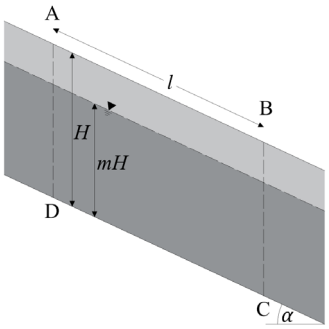

Figure 1. Model of an infinite slope.

The accelerations in the *x-y* plane are resolved into components normal, $a'_{\mathrm{N}}(t)$, and tangential, $a'_{\mathrm{T}}(t)$, to the sliding surface, i.e., in the T-N plane, as given by Equations (1) and (2):

$$a'_{\mathrm{N}}(t) = a'_x(t)\sin(\alpha) + a'_y(t)\cos(\alpha) \quad (1)$$

$$a'_{\mathrm{T}}(t) = a'_x(t)\cos(\alpha) - a_{y'}(t)\sin(\alpha) \quad (2)$$

Assuming the sliding resistance follows the Mohr-Coulomb failure criterion, the transient factor of safety $\mathrm{FoS}(t)$ against sliding for the free-body diagram in Figure 2b can be expressed following the formulation by Ingles, Darrozes and, Soula (2006):

$$\mathrm{FoS}(t) = \frac{g\left(\frac{c'}{H\cos\alpha} - m\,\gamma_{\mathrm{w}}\cos\alpha\tan\phi\right)}{\gamma\,(a'_{\mathrm{T}}(t) + g\sin\alpha)} + \frac{(g\cos\alpha - a'_{\mathrm{N}}(t))\tan\phi}{a'_{\mathrm{T}}(t) + g\sin\alpha} \quad (3)$$

where g denotes the gravitational acceleration, γ is the unit weight of the soil, H is thickness of the sliding mass, m corresponds to the ratio between the depth of the phreatic level and H, γ_w is the unit weight of water, α is the slope inclination, ϕ is the soil's internal friction angle, and c represents the soil cohesion. When $\mathrm{FoS}(t) = 1$, the system reaches the onset of failure. From this condition, the critical tangential acceleration $a_{\mathrm{Tc}}(t)$ can be derived as:

$$a'_{\mathrm{Tc}}(t) = g\left[\frac{c}{\gamma\,H\cos\alpha} + \left(1 - \frac{m\,\gamma_{\mathrm{w}}}{\gamma}\right)\cos\alpha\tan\phi - \sin\alpha\right] - a'_{\mathrm{N}}(t)\tan\phi \quad (4)$$

Equation (4) provides a time-dependent critical acceleration that accounts for both the mechanical properties of the system and variations in normal stress due to seismic loading. Figure 6 illustrates the relationship between the normal inertial acceleration $a'_{\mathrm{N}}(t)$ and the critical tangential acceleration $a'_{\mathrm{Tc}}(t)$. When $a'_{\mathrm{N}}(t)$ is positive, it reduces the contact force by tending to separate the block from its base, thus lowering $a'_{\mathrm{Tc}}(t)$. Conversely, negative values of $a'_{\mathrm{N}}(t)$ increase the contact force, resulting in greater resistance and therefore a higher $a'_{\mathrm{Tc}}(t)$.

2.2 *Double integration scheme*

The algorithm proposed by Wilson and Keefer (1983) employs an adaptive explicit trapezoidal scheme to integrate segments of the acceleration time history that exceed the yield threshold, continuing until the relative velocity of the block is reduced to zero. This process yields a velocity time history, which is then integrated to compute the accumulated permanent displacement.

The original formulation is consistent with Newmark's approach. Hence, in this work, the scheme is adapted to address the limitations previously discussed. The key modifications are the use of the tangential inertial acceleration time history, $a'_{\mathrm{T}}(t)$, in place of the horizontal ground acceleration $a_{\mathrm{x}}(t)$, and the adoption of a time-dependent yield threshold, $a'_{\mathrm{Tc}}(t)$, instead of a constant value. The implementation of the scheme involves:

1. Compute the normal and tangential inertial acceleration time histories, $a'_{\mathrm{N}}(t)$ and $a'_{\mathrm{T}}(t)$, using Equations (1) and (2).
2. Evaluate the time-varying yield threshold $a'_{\mathrm{Tc}}(t)$ using Equation (4).
3. Integrate segments of $a'_{\mathrm{T}}(t)$ that exceed $a'_{\mathrm{Tc}}(t)$, continuing until the relative velocity of the block becomes zero.
4. Integrate the resulting relative velocity time history to compute the permanent displacement.

2.3 *Incorporation of directionality effects*

To account for the effect of horizontal directionality, the rotational approach, proposed by Pinzón et al. (2020), is adopted. This method involves performing a series of analyses by gradually rotating the slope around a fixed vertical axis. For a given azimuthal orientation θ, the rotated horizontal acceleration components, $a_{x1}(t,\theta)$ and $a_{x2}(t,\theta)$, are obtained by applying a linear transformation to the original recorded components, $a_{\mathrm{EO}}(t)$ and $a_{\mathrm{NS}}(t)$:

$$\begin{bmatrix} a_{x1}(t,\theta) \\ a_{x2}(t,\theta) \end{bmatrix} = \begin{bmatrix} \cos\theta & \sin\theta \\ -\sin\theta & \cos\theta \end{bmatrix} \begin{bmatrix} a_{\mathrm{EO}}(t) \\ a_{\mathrm{NS}}(t) \end{bmatrix} \text{ for } \theta \in [0, l] \quad (5)$$

where θ is the azimuthal rotation angle, and l defines the upper bound of the rotation range to be evaluated.

Given the inherent asymmetry of slopes, the full azimuthal range, $\theta \in [0, 360]$, is considered. In two-dimensional analyses, only one of the rotated components is applied as the input motion (a_{x1}). To reduce the computational cost of the analyses, a rotation interval of 3° is employed, which provides a reasonable balance between resolution and calculation time. This approach enables a comprehensive evaluation of how the slope response varies with azimuthal orientation. It also allows for a direct identification of the orientation associated with the maximum response, referred to as the critical angle θ_{crit}.

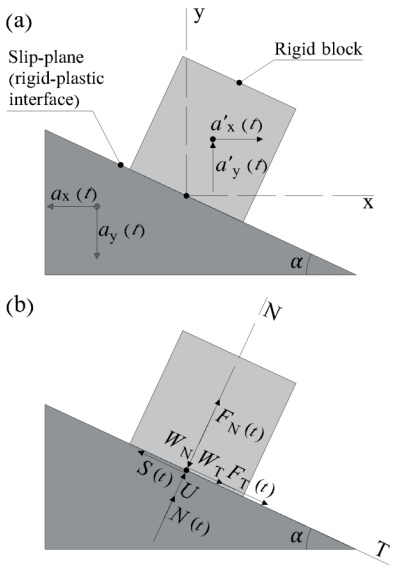

Figure 2. (a) Inertial acceleration acting on the rigid-block model and (b) free-body diagram of the rigid block under bidirectional loading in the T–N plane.

3 ANALYSIS PROCEDURE

3.1 *Model configurations*

To evaluate the performance of the proposed model in comparison with other rigid-block approaches, three configurations are analysed. Model A follows the traditional Newmark method, in which the horizontal acceleration is applied tangentially to the sliding surface and the vertical component is neglected. Model B employs the bidirectional loading framework but includes only the horizontal seismic component. Model C extends this formulation by incorporating both horizontal and vertical seismic components. These three configurations are illustrated in Figure 3.

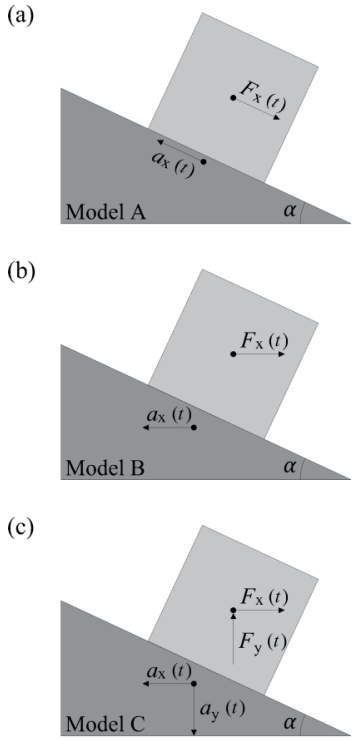

Figure 3. Rigid-block models studied: (a) Model A, horizontal ground motion component parallel to the slope (Newmark's model); (b) Model B, horizontal ground motion component only and (c) Model C, horizontal and vertical ground motion components.

To reflect a representative range of slope conditions, the analysis begins with a base case, and then the key parameters controlling stability conditions are varied systematically; in particular, the slope inclination and shear strength, defined by the soil's friction angle and cohesion, are varied. These parameters are modified within realistic bounds to ensure relevance. The full set of values adopted is summarised in Table 1. A deep phreatic level is assumed in all cases to avoid complexities associated with dynamic pore pressure generation.

Table 1. Slope parameters.

Parameter	Symbol	Range	Unit	No. of values
Slope inclination	α	38-54	º	5
Friction angle	ϕ	30-38	º	5
Cohesion	c'	15-25	kPa	5
Unit weight	γ	20	kN/m^3	1
Thickness	H	3	m	1
Ratio of phreatic level to thickness	m	0	-	1

3.2 *Input motions*

To evaluate a wide range of seismic scenarios, i.e., motions with different vertical-to-horizontal peak ground acceleration ratios (VPGA/HPGA) and directionality effects, a total of 112 sets of three-component ground motion records were selected from the PEER NGA database (Ancheta *et al.*, 2013). These records come from multiple seismic events, several of which are known to exhibit directivity and fling-step effects. Only records measured on firm ground (shear wave velocity exceeding 500 m/s) were included. The selected events are listed in Table 2.

Table 2. Selected seismic events.

Earthquake	Location	Year	Moment magnitude
San Fernando	United States	1971	6.61
Irpina	Italy	1980	6.90
Coalinga	United States	1983	6.36
Morgan Hill	United States	1984	6.19
Loma Prieta	United States	1989	6.93
Northridge	United States	1994	6.69
Kobe	Japan	1995	6.90
Kocaeli	Turkey	1999	7.51
Chi-Chi	Taiwan	1999	7.62

Figure 4 shows the distribution of VPGA/HPGA as a function of rupture distance (R_{RUP}) for all records, including mean values and the full range of variation across azimuthal orientations. Although VPGA/HPGA exhibits fluctuations at all rupture distances, a mild correlation is observed, with the highest ratios occurring within 15 km of the fault.

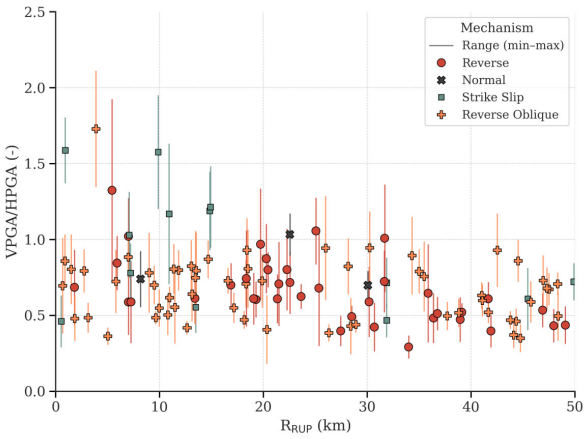

Figure 4. Distribution of the VPGA/HPGA ratio as a function of rupture distance for the dataset selected.

3.3 *Scaling procedure*

Due to the variability of the critical acceleration of the different slope configurations, defining a single seismic intensity level may result in responses either null or extreme (beyond realistic values that a slope can withstand without losing strength and collapsing). To address this, a demand-based scaling approach is used. Its goal is to reduce dispersion in the responses and constrain displacement values to realistic levels. The demand parameter DP is defined as the ratio between the system's base critical acceleration and a representative horizontal ground motion intensity:

$$DP = \frac{a'_{Tc}(t=0)}{RotD50_{T=0s}} \quad (6)$$

where $a'_{Tc}(t=0)$ is the base critical acceleration (unaffected by induced seismic forces), and $RotD50_{T=0s}$ is the 50th percentile of the rotated peak horizontal ground accelerations over azimuthal rotations between 0° and 180° (Equation (7)).

$$RotD50_{T=0s} = \text{percentile}_{50}[\max|a_{rot}(t,\theta)|] \text{ for } \theta \in [0,180] \quad (7)$$

The scaling procedure consists of computing a scale factor (SF) that adjusts each ground motion record to reach a predefined demand level, DP_{target}, for each system configuration. This factor is calculated as:

$$SF = \frac{a'_{Tc}(t=0)}{RotD50_{T=0s} \cdot DP_{target}} \quad (8)$$

All three components of each record are scaled by this factor, preserving the original directional characteristics of the motion.

To determine a suitable value for DP_{target}, a preliminary calibration is performed using a subset of records. A displacement of 15 cm is chosen as the reference limit state, representing the threshold beyond which permanent deformations may lead to significant damage (Jibson, 2011). For the base configuration, a value of DP_{target} = 0.35 yields a 50th percentile of displacements closely matching this reference level.

It is important to emphasise that, although a reference value of DP_{target} = 0.35 is used for scaling, the actual demand experienced by the system still depends on the azimuthal orientation. Because the scaling is anchored to the $RotD50_{T=0s}$, orientations other than the one associated with this measure will exhibit different demand levels (in terms of the ratio between the critical base acceleration and the peak ground acceleration).

4 INFLUENCE OF THE VERTICAL COMPONENT ON PERMANENT DISPLACEMENTS

To assess the influence of the vertical component on the slope response, Models B and C are compared. Figure 5a presents the displacements obtained using Model B (*x*-axis) versus those obtained using Model C (*y*-axis), considering only the cases where displacements range from 0.01 to 0.50 m. Although the dispersion increases with the magnitude of displacements, the results tend to cluster around the 1:1 line, suggesting that the inclusion of the vertical component in Model C produces, on average, similar results to those from Model B, which neglects it.

A closer analysis of specific cases where the consideration of the vertical component influences the response yields additional insights. When the differences between Models B and C are negligible, two typical conditions tend to apply: either the vertical acceleration exhibits low amplitude and high frequency, limiting its impact, or the vertical and horizontal pulses are out of phase, reducing their interaction. In contrast, when the horizontal and vertical pulses are in phase and the horizontal pulse occurs in the downslope direction, the vertical component has a higher probability of influencing the block's response. In such cases, the direction of the vertical inertial force plays a crucial role in determining whether its effect is stabilising or destabilising.

Figure 6 helps illustrate this behaviour through two simplified examples in which a rigid block is subjected to simultaneous horizontal and vertical inertial acceleration pulses. In Figure 6a, an upward vertical pulse reduces both the tangential driving force and the normal force acting on the block. For the given system configuration (in terms of geometry and mechanical parameters), the reduction in driving force prevails over the reduction in resistance, resulting in smaller displacements compared to Model B, which neglects this effect. Such cases correspond to points below the 1:1 line in Figure 5a.

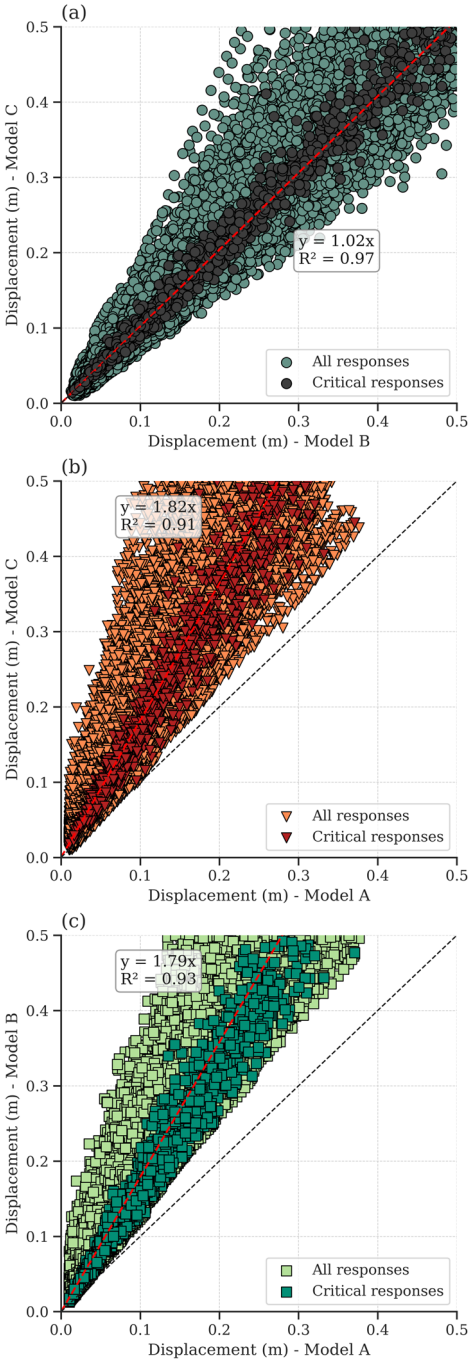

Figure 5. Comparison of the response in terms of permanent displacements for the different models: (a) Model C vs. Model B, (b) Model C vs. Model A, and (c) Model B vs. Model A.

Conversely, as shown in Figure 6b, when the vertical inertial acceleration acts downward, it increases both the driving tangential force and the normal force. However, the stabilising effect of the increased normal force is insufficient to compensate for the increased driving force, reducing overall stability. As a result, Model C predicts larger displacements than Model B, and these cases appear above the 1:1 line in Figure 5a.

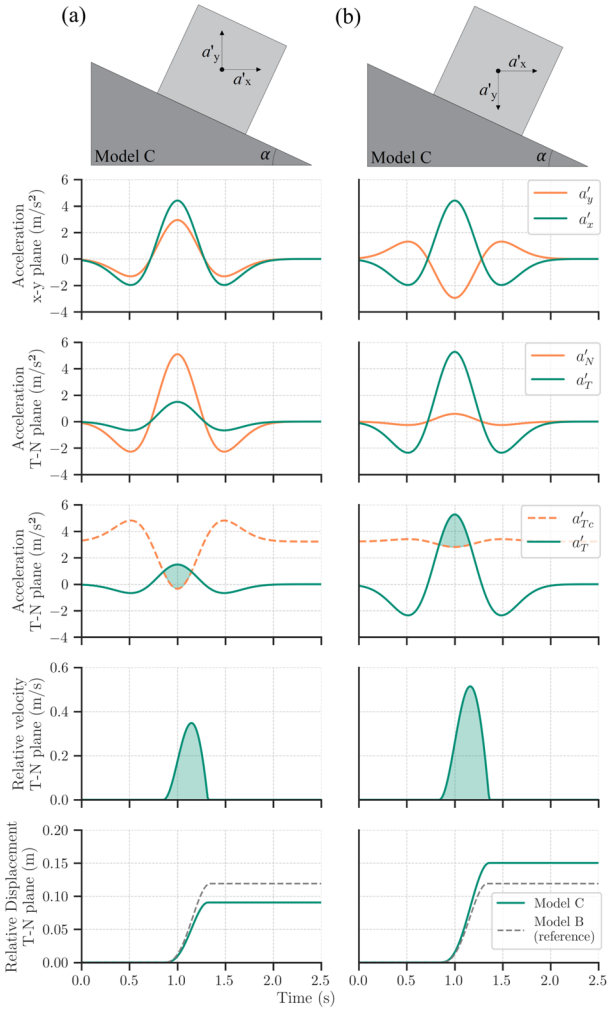

Figure 6. Comparison of Model C responses (with $\alpha = 40°$, $\phi = 35°$, $c = 20$ kPa, $H = 3$ m, $\gamma = 20$ kN/m^3, $m = 0$) to a horizontal Ricker pulse ($A = 0.45$ g, $f = 0.8$ Hz) and a vertical Ricker pulse ($A = 0.30\,g$, $f = 0.8$ Hz) in two cases: (a) upward vertical pulse, and (b) downward vertical pulse. The displacements of Model B are presented as reference.

Taken together, the results indicate that the vertical component is generally not a dominant factor in slope stability analysis, as evidenced by the overall clustering of data around the 1:1 line in Figure 5a. However, there are specific conditions under which the vertical component has a notable effect. In these cases, its net influence depends on the geometry of the slope, the material properties, and the seismic motion characteristics, particularly amplitude, frequency content, and, most importantly, the phase relationship between pulses in different directions.

On the other hand, Figure 5b compares the displacements predicted by Models A and C. The slope of the trend line, 1:1.82, indicates that Model A significantly underestimates displacements relative to Model C. Importantly, this underestimation is not due to the absence of the vertical component in Model A, but rather to neglecting the variations in resistance caused by fluctuations in the normal force. This conclusion is further supported by the comparison between Models A and B in Figure 5c, where the vertical component is not considered. Here, the trend line has a slope of 1:1.79, closely matching the previous comparison. The main difference is that this comparison exhibits somewhat lower dispersion, likely due to the absence of the vertical component.

5 INFLUENCE OF THE VERTICAL COMPONENT ON THE ORIENTATION OF MAXIMUM RESPONSE

Figure 7 compares the critical orientations obtained using the different models. In Figure 7a, the effect of vertical motion is evaluated through the comparison of Models B and C. A clear trend is observed where the responses tend to cluster along the 1:1 line. This indicates that, in most cases, the critical orientation is not substantially affected by the consideration of the vertical motion component. This behaviour reflects the dominant role played by the horizontal component in the response of rigid-block systems.

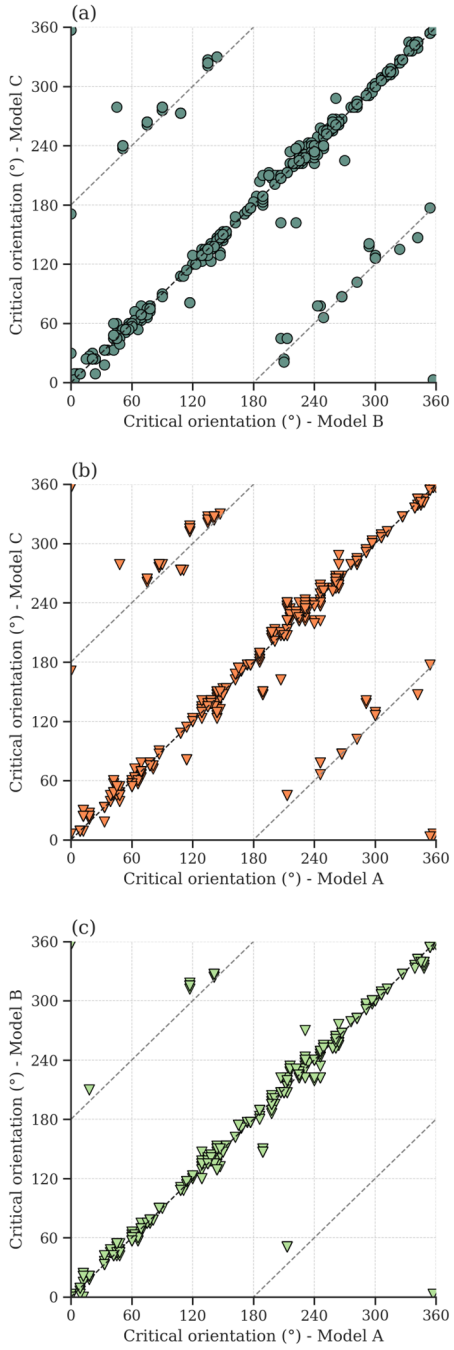

Figure 7. Comparison of the critical orientation obtained for the different models: (a) Model C vs. Model B, (b) Model C vs. Model A, and (c) Model B vs. Model A.

The predominance of the horizontal motion is further evidenced by the results shown in Figure 5. The responses associated with the critical orientation of each case are highlighted. These

responses are mostly concentrated near the 1:1 line of the plot, and their spread does not seem to increase with larger displacements. This behaviour suggests that, at the critical orientation, the inclusion of the vertical component does not substantially affect the system's response. A plausible explanation is that the horizontal motion tends to be maximised at the critical orientation for all records, thereby reducing the relative contribution of the vertical component to the overall stability.

Nonetheless, there are specific cases where a polarity shift occurs in the critical orientation. This is evident from the appearance of points aligned along two lines parallel to the 1:1 line, which correspond to cases where the critical orientation in Model C differs by 180° from that in Model B. These polarity shifts are associated with nearly symmetric response variation patterns, in which the system's sensitivity to orientation varies around a principal axis. In such cases, the symmetry of the response promotes conditions where even small changes in the input motion (e.g., considering the vertical acceleration component) can lead to a 180° shift in the critical orientation.

Figure 7c shows the comparison between Models B and A. In this case, the number of polarity shifts is significantly reduced, supporting the hypothesis that such shifts are primarily driven by the inclusion of the vertical motion component. Nevertheless, the overall results suggest that the principal axis of critical orientation remains largely unaffected by the model used or by the inclusion of the vertical component.

6 CONCLUSIONS

This study aimed to understand how the vertical component of seismic motions affects the response of slopes, and how its consideration, commonly disregarded for simplicity, interacts with directionality. To that end, a comparative analysis was performed using simplified rigid-block-type representations.

The response in terms of permanent displacements was evaluated for three models. Model A corresponds to Newmark's original proposal. Models B and C represent modified formulations designed to account for the influence of seismic motion on both the driving force and the shear resistance at the sliding interface. The difference between them lies in the fact that Model B considers only the horizontal seismic component, while Model C includes both horizontal and vertical components in the calculation.

To assess the influence of directionality on the response of slopes under varying input motions (i.e., different frequency content and directionality effects), 112 sets of accelerograms were used. These records were selected according to specific criteria and included both near-field and far-field motions. Regarding the slope properties, different parameter combinations were evaluated, with values representative of the failure mechanisms of interest. Additionally, a demand-based scaling strategy was proposed and applied to reduce dispersion and to constrain displacements to realistic levels for the type of systems analysed.

The results indicate that the horizontal component generally dominates the slope response, with the vertical component playing a secondary role. In most cases, the vertical input only slightly modifies the displacement magnitude, although there are cases where its effect becomes significant. In those cases, the vertical component may either increase or reduce displacements, with a modest tendency toward larger values. The net effect is governed by the slope's geometric and mechanical properties, as well as the phase relationship between acceleration pulses in different directions. The proposed models allow for straightforward identification of cases in which the characteristics of both the system and the site's seismic environment meet the conditions under which the vertical component becomes relevant and has to be accounted for in the stability assessment.

Regarding the comparison between the more rigorous formulations and Newmark's model, it was observed that the latter, due to its simplified treatment of seismic loading, neglects variations in the contact force at the sliding interface. As a result, it tends to underestimate displacements compared to models that explicitly account for this effect.

Finally, regarding the orientation of the maximum response, the results show that, in most cases, it is not affected by the consideration of the vertical component. However, in specific instances, the vertical motion can trigger a polarity shift in the critical direction, corresponding to a 180° rotation. These shifts are more likely to occur in ground motions that exhibit a highly symmetrical response pattern with respect to orientation. Nevertheless, the main axis of critical orientation remains consistent regardless of the rigid-block model adopted or the inclusion of the vertical component.

7 ACKNOWLEDGEMENTS

This study was supported by The National Secretariat of Science, Technology and Innovation of the Republic of Panama (SENACYT) (grant number 063–2025).

8 REFERENCES

Ancheta, T. et al. (2013) PEER NGA-West2 database. Pacific Earthquake Engineering Research Center. Available at: https://ngawest2.berkeley.edu/

Du, W. (2018) 'Effects of directionality and vertical component of ground motions on seismic slope displacements in Newmark sliding-block analysis', Engineering Geology, 239, pp. 13–21. Available at: https://doi.org/10.1016/j.enggeo.2018.03.012.

Gazetas, G., Garini, E. and Georgarakos, T. (2009) 'Effects of Near-Fault Ground Shaking on Sliding Systems', Journal of geotechnical and geoenvironmental engineerin, 135(12), pp. 1906–1921.

Ingles, J., Darrozes, J. and Soula, J. (2006) 'Effects of the vertical component of ground shaking on earthquake-induced landslide displacements using generalized Newmark analysis', Engineering Geology, 86(2–3), pp. 134–147. Available at: https://doi.org/10.1016/j.enggeo.2006.02.018.

Jibson, R. (2011) 'Methods for assessing the stability of slopes during earthquakes-A retrospective', Engineering Geology, 122(1–2), pp. 43–50. Available at: https://doi.org/10.1016/j.enggeo.2010.09.017.

Korzec, A. and Jankowski, R. (2021) 'Extended Newmark method to assess stability of slope under bidirectional seismic loading', Soil Dynamics and Earthquake Engineering, 143. Available at: https://doi.org/10.1016/j.soildyn.2021.106600.

Kramer, S. and Lindwall, N. (2004) 'Dimensionality and Directionality Effects in Newmark Sliding Block Analyses', Journal of Geotechnical and Geoenvironmental Engineering, 130(3), pp. 303–315. Available at: https://doi.org/10.1061/(ASCE)1090-0241(2004)130:3(303).

Morales, A., Manica, M. and Pinzon, L. (2024) 'Slope stability under seismic actions considering directionality effects', in 8th international conference on earthquake geotechnical engineering. Osaka, Japan: Japanese Geotechnical Society.

Newmark, N. (1965) 'Effects of Earthquakes on Dams and Embankments', Géotechnique, 15(2), pp. 139–165. Available at: https://doi.org/https://doi.org/10.1680/geot.1965.15.2.139.

Pinzón, L. et al. (2020) 'Dynamic soil-structure interaction analyses considering directionality effects', Soil Dynamics and Earthquake Engineering, 130. Available at: https://doi.org/10.1016/j.soildyn.2019.106009.

Wilson, C. and Keefer, D. (1983) 'Dynamic analysis of a slope failure from the 6 August 1979 Coyote Lake, California, earthquake', Bulletin of the Seismological Society of America, 73(3), pp. 863–877. Available at: https://doi.org/10.1785/BSSA0730030863.